17th World Conference on Earthquake Engineering, 17WCEE
Sendai, Japan - September 13th to 18th 2020

FREQUENCY CONTENT IN STOCHASTIC GROUND MOTION SIMULATIONS AND OBSERVED DATA FOR ROCK SITE CONDITIONS

L.G Alvarez Sanchez [1], I. Zentner [2], L.F. Bonilla [3], G. Senfaute [4]

[1] *PhD Student, EDF R&D, IUSS-Pavia, IFSTTAR, luis.alvarez@iusspavia.it*
[2] *Research Engineer, EDF R&D, irmela.zentner@edf.fr*
[3] *Research Director, IFSTTAR, luis-fabian.bonilla-hidalgo@ifsttar.fr*
[4] *Research Engineer, EDF R&D, gloria.senfaute@edf.fr*

Abstract

Stochastic Ground Motion Simulation Methods (SGMSM) represent an attractive alternative to obtain acceleration records for structural analysis when dealing with incomplete earthquake databases or when very rare events, corresponding to extreme seismic scenarios, have to be considered in safety analyses.

Considering the advantages and ever-increasing prediction capacity of time history analysis, dynamic characteristics of ground motions, such as the evolution of the frequency content, become paramount features for valid SGMSM. Based on this premise, the main objective of this study is to evaluate the capacity of SGMSM to capture the observed frequency content of ground motion. To achieve such goal, we employed the recently developed Otarola et al SGMSM [1] [2], which offers a physical approach to model of the complete body-wave field. To complement the original method, we included the recently developed inter-frequency correlation structure [3], defined from the analysis of recorded ground motion, in the computation of the different Fourier Amplitude Spectra.

The evaluation of the frequency content was performed by comparison of the Smoothed Fourier Amplitude Spectra (SFAS), and the instantaneous frequency of observed signals with that of their correspondent simulations. The assessment was focused on ground motions at rock site, to eliminate the impact local site effect. First, sensitivity analyses are performed to detect the most important physical parameters driving the model; subsequently a machine learning aided algorithm was employed to find the best source and propagation parameters of the defined case study.

Results indicate that the modified Otarola method can capture the mean frequency content of the observed database. As expected, the inter-frequency correlation structure was found to be key for a proper modeling of instantaneous frequency of simulated ground motion.

Keywords: Frequency evolution, Stochastic Ground Motion Simulation

1. Introduction

Stochastic Ground Motion Simulation Methods (SGMSM), such as those described by authors like Boore [4] [5] [6] and more recently Otarola [1] [2], have drawn the attention of the engineering community due to their capacity to mimic seismic ground motion features at little computational effort, in comparison with other more complex Ground Motion Simulation methods. Such promising capacity gains special importance in places where certain seismic scenarios of interest have not yet been seen nor measured.

Most studies on SGMSM have focused on assessing only the capacity of the methods to reproduce simple engineering quantities such as the response spectrum or the Fourier Amplitude Spectrum (FAS) of reference signals. However, considering the increasing widespread use of time history analysis, characteristics such as the evolution of the frequency content also become key features in the validation of SGMSM to be used in the design and assessment of structures.

On the same note, the SGMSM have evolved in recent years. Studies such as those conducted by Bayless et al [7] [3], based on the analysis of recorded ground motion databases, have proved the existence of a correlation structure relating the amplitude of the motion at different frequencies. Moreover, their work has shown the impact on fragility curves computed with SGMSM assuming non-correlated noise. To correct this deficiency, and as part of their results, the authors proposed empirical models, ready to be included in SGMSM, allowing to include the natural tendencies noted in the frequency content of ground motion.

Amongst the most recently developed SGMSM is that of Otarola et al [1] [2]. The method was developed with the intention of capturing more accurately the high energy seismic events produced in the Chilean subduction zone. The main difference of this method compared to EXSIM [6] is the modelling of the complete body-wave field by including the P and SV-waves.

It is the intention of this study to analyze the frequency content of ground motions simulated with the Otarola method [1] [2] when, accounting for the correlated inter-frequency content as noticed in recorded ground motions. The assessment is focused on rock sites, to eliminate the impact local site effect. First, sensitivity analyses are performed to detect the most important physical parameters driving the model; subsequently a machine learning aided algorithm was employed to find the best source and propagation parameters of the defined case study. Finally, the frequency content of the simulated signals was compared with the one from the recorded ground motion.

2. Methodology

2.1) Stochastic Ground Motion Simulation (SGMS)

SGMS was performed employing the model proposed by Otarola [1] [2]. We modified their model to further include the inter-frequency correlation structure of recorded ground motion as proposed by Bayless [3].

Based on previous stochastic models such as those described and compared by Boore [4] [5] [6], ground motions are assumed to be produced by the lagged summation (modelling their travel time from the source to the site of interest), of the acceleration time histories, produced by an array of Brune point sources used to discretize the ruptured fault.

Ground motion from each point source, or sub-fault, are computed by modelling the FAS of the seismic waves. One of the main distinctions of the Otarola method from previous stochastic ground motions simulation methods, such as EXISM or FINSIM [6], is that it models the full body-wave field of the motion, including not only the most energetic SH-waves but also the P and SV-waves, of great importance for records registered close to the source or from subduction areas. Furthermore, the inclusion of the full body wave field allows the Otarola method to produce signals in the three main orthogonal components (i.e. North – South, East – West, Up-Down).

The Otarola method follows the same general approach as that proposed for SH-waves by Boore [4] [5] [6]. A convolution of filters representing the source, path and site (herein defined as underlying spectrum) is applied to a normalized Power Spectral Density (PSD) white noise defined for each sub-fault.

To properly aggregate the signals from the different body-waves, the underlying FAS are computed for a coordinate system composed of radial, tangential and vertical components. The computation of the Brune underlying spectrum $A_i^w{}_d(f)\ A_i^w{}_d(f)$ for each sub-fault "i", body-wave type w (P, SV and SH) and component d (radial, tangential and vertical, r, t and z respectively) is described in equation (1):

$$A_i^w{}_d(f) = 4\pi^2 f^2\ E(f)P(r_i,f)S(f) \tag{1}$$

Where $E(f)\ E(f)$ refers to the source, $P(r_i,f)\ P(r_i,f)$ to the path and $G(f)\ G(f)$ to the site.

$$E(f) = \frac{M_{0_i}(R^w{}_i\ FS^w{}_i\ EP^w{}_i)}{4\pi\rho_i {v_i}^3}\ \frac{(2\pi f)^2}{1+\left(\frac{f}{f_c^w{}_i}\right)^2} \tag{2}$$

The source is defined by $M_0 M_0$ which refers to the sub-fault seismic moment; $R^w{}_i R^w{}_i$ are the analytical radiation coefficients; $FS^w{}_i\ FS^w{}_i$ are the amplification factors due to the free surface ; $EP^w{}_i\ EP^w{}_i$ are the factors modeling the energy partition of the body-waves into the radial, tangential and vertical components; $v_i v_i$ refers to the body-waves velocities; $f_c^w{}_i f_c^w{}_i$ is the dynamic corner frequency of the sub-fault.

$$P(r_i,f) = G(r_i)\exp\left(-\frac{\pi f r_i}{Q^w(f)v_i}\right) \tag{3}$$

The path component of the simulation is described in equation (3). The function $G(r_i)\ G(r_i)$ represents the geometrical spreading depending on a reference distance from the finite point source to the site of interest, for this study this function is assumed to be described by the following function:

$$G(r_i) = r_i^b \tag{3}$$

The total travelled distance including the refraction of the direct rays due Snell's law was considered as reference for this study $(r_i)\ (r_i)$. The quality factors for each of the body-waves are represented by the function $Q^w(f)\ Q^w(f)$.

$$S(f) = \exp(-\pi f\kappa_0)\ a(f) \tag{4}$$

As per Boore [5], the site effect represented in equation (4) is separated into an attenuation and an amplification effect. The attenuation operator accounts for the path independent attenuation of high frequency content, considered in this application with the $\kappa_0\kappa_0$ filter. The amplification $a(f)a(f)$ could be computed based on different functions or models; this study employs an empirical amplification model developed for a Japanese reference generic rock site ($V_{s30} > 760\ m/sV_{s30} > 760\ m/s$) [8].

Since the method includes the computation of different body-wave types, the generic assumption of a vertical incidence angle employed by Boore [4] [5] [6] for the SH waves simulation is no longer necessary; in fact the method relies on the geometrical propagation of the seismic waves to compute the free surface factors $FS^w{}_i\ FS^w{}_i$ and to aggregate the acceleration time histories into the commonly employed orthogonal components. Such exercise was conducted considering direct rays propagating through a 1D layering model, described by the shear wave velocity of the soil layers, bearing in mind the refraction of the rays by Snell's law.

Originally, the method developed by Otarola [1] [2] employs windowed common Gaussian white noise as a representation of the stochastic behavior of ground motion frequency content, nevertheless, as pointed out by some studies [9] [10], residuals (ε) FAS, obtained from natural ground motion databases and Ground Motion Models (GMM), at different frequencies are correlated. The correlation coefficient (ρ) decreases as the distance between frequencies increases.

Accounting for this ground motion feature in SGMSM is of interest for engineering purposes since inter-period response spectrum correlation directly affects structural response of Multi-Degree of Freedom Systems (MDOF). Without the adequate correlation structure imbedded in the simulation process of ground motions, variability in the structural response may be underestimated it, leading to non-conservative estimates of seismic risk [3].

Some authors such as Bayless [3] have employed recent ground motion databases and common GMM's to derive expressions describing the noted correlation structure in the response spectrum (which is worth mentioning, does not seem to be region, distance nor magnitude dependent). This representation however, "provides the peak response from a single degree of freedom system, which is influenced by a range of frequencies, and the breath of that range is dependent on the oscillator period" [7]. Under this reasoning Bayless et al [7] suggest a more direct modelling of this correlation through the linear representation of the Fourier Amplitude Spectrum (FAS) of the signals.

Recent efforts have yielded both a GMM for FAS as IM and a residual correlation structure based on the latter. We opted for the use of correlated noise, using the previously described inter-frequency correlation structure proposed by Bayless [7].

It is not the intention of this paper to fully cover the method developed by Otarola, but to explain the notions supporting it; for further study the reader is referred to studies solely devoted to the method and its application, such as [1] [2].

2.2) Frequency content in ground motions

In this specific study, the frequency content of ground motions was analyzed by means of the SFAS and the instantaneous frequency of the signal through time ($\tilde{f}$).

The SFAS depicts the overall frequency content of the entire signal. Smoothing of the signals was used to facilitate the analysis and comparison of the frequency content of different signals. To this end, the Konno Ohmachi smoothing technique was applied, [11], considering a constant bandwidth parameter $b = 40$. Figure 1 shows an example of the SFAS of a common signal

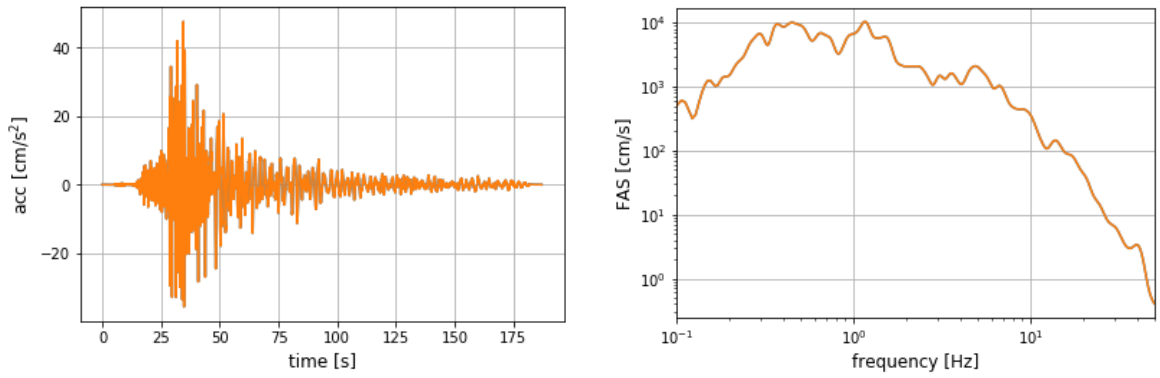

Fig. 1 - (a) Acceleration time series - (b) SFAS of the signal presented in (a)

The evolution of the frequency content in ground motion, or instantaneous frequency, was defined based on the central frequency ($\tilde{f}$) of a sliding window moving across the signal. The latter indicates the predominant frequency within a given time window and is computed as the weighted average of the Fourier Amplitude Spectrum.

$$\tilde{f} = \frac{\sum_f f\ SFAS(f)}{\sum_f SFAS(f)} \tag{5}$$

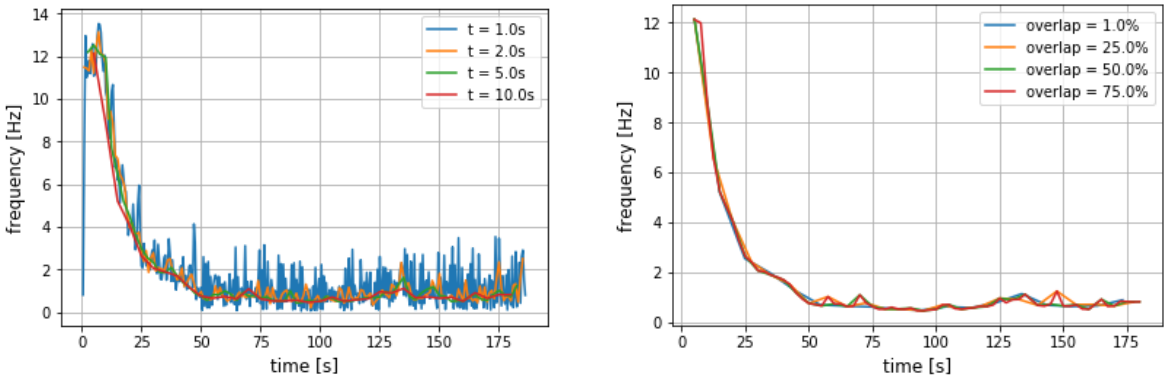

(a) (b)

Fig. 2 - (a) Window size effect in the computation of the instantaneous frequency (constant overlap of 50%) - (b) Overlapping percentage effect in the computation of the instantaneous frequency (constant window size of 5s)

The instantaneous frequency of the signal shown on Figure 1 is presented in Figure 2. The impact of both parameters defining the analysis window is also shown in the latter figure. If a small window size is set, the instantaneous frequency will be more reactive to the small variations in the frequency content of the signal; closer to the exact frequency content per time step though presenting a much noisier estimation. The overlapping percentage provides continuity in the instantaneous frequency estimation at instants where large differences might be expected, such as the arrival of *S-waves*.

Aiming for a smooth instantaneous frequency function, a constant setup of a 5.0 seconds sliding window and overlapping of 50% was considered for all analyses performed. Since the purpose of this study is to evaluate only of the frequency content of the seismic waves, the initial part of the signals not containing any seismic input was cut using an Arias-intensity based criterion. As a consequence, only the part of the signal between the values of 0.1 % and 99.9% of the total Arias energy is considered. For easiness in the comparison of the frequency content of signals with different lengths we normalized the time of the cropped signals, so each ranges from 0.0 at the beginning to 1.0 at the end.

3. Application - Study case

The reference data used in this study was obtained from the Japanese KiK-net seismic network [12]. A total of 10 ground motions (composed of three component accelerograms), produced by events with a moment magnitude (M_w (M_w) ranging between 6.1 and 7.2, and measured in rock based stations ($V_{s30} \geq 800.0\ m/s V_{s30} \geq 800.0\ m/s$) were selected. A description of the set of events used as reference, and the S-wave and P-wave velocity profiles for each station are presented Table 1and Figure 3, respectively.

Table 1 – Reference record set

Id	*Station*	M_w	R_{hyp} $[km]$	PGA $[^{cm}/_{s^2}]$	*Date*
FKSH07-01	FKSH07	6.3	16.30	105.30	25/02/13
FKSH07-02	FKSH07	6.5	60.93	121.85	23/10/04
FKSH07-03	FKSH07	6.1	45.82	120.70	27/10/04
FKSH15-01	FKSH15	7.2	197.97	8.60	16/08/05
FKSH15-02	FKSH15	6.8	119.80	14.02	23/10/04
FKSH15-03	FKSH15	7.0	197.94	8.07	26/05/03
TCGH17-01	TCGH17	6.8	116.63	24.37	16/07/07
TCGH17-02	TCGH17	6.8	81.60	66.47	23/10/04
TCGH17-03	TCGH17	6.3	27.97	36.35	25/02/13
TCGH17-04	TCGH17	6.1	69.07	45.80	27/10/04

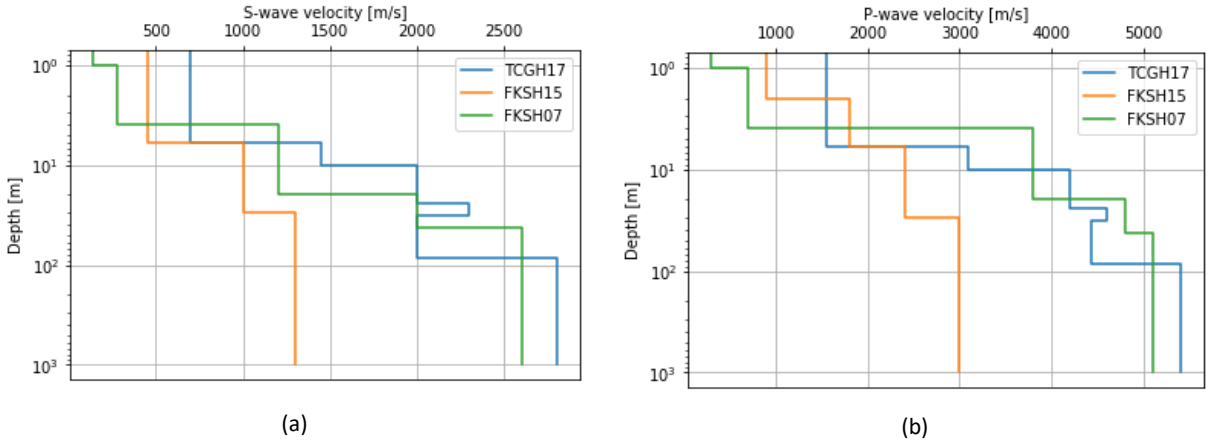

(a) (b)

Fig. 3 – (a) S-wave velocity profiles for the studied stations - (b) P-wave velocity profiles for the studied stations

The raw records where post-processed to eliminate any baseline produced by high noise content in the low-frequency range of the signals, [13]. A low-cut Butterworth filter (high-pass filter) was applied to the signals, selecting a constant filter order of 3 and a corner frequency of 0.1 Hz. The selection of the filter frequency was based on the analysis of the noise-to-signal ratio of the accelerograms, as recommended in the literature [13]. Since the low-cut filter is applied to very low frequencies, affecting mainly the initial part of the signal before any seismic wave arrival, we expected no influence in the evaluation of the frequency content of the actual signal containing the ground motion.

3.1) SGMSM parameter identification

The selected array of reference events was considered to be part of a regional seismic environment, in other words, we assume that all reference events were produced by a single set of SGMSM physical parameters. Based on the previous assumption, we considered the calibration of the method as the identification of the physical variables rendering the smoothed mean simulated FAS ($\widetilde{SFAS}_{sim}$) closest to that of the reference events ($SFAS_{ref}$).

- Sensitivity analysis

Identification of the most influential SGMSM physical variables was conducted through a sensitivity analysis. Latin Hypercube Sampling (LHS) was used to design an experiment consisting of 50 subjects, each a set of the physical variables characterizing the source, propagation and site filters defined in equations *(2)*,

(3) and *(4)*. The variables selected for the analyses where: stress drop (σ), kappa (κ), pulsing percentage of the fault (ζ) and the geometric spreading function (b) (represented through the exponent of applied to the reference distance (r_i). A total of 50 simulations were carried out for each experiment subject, registering the SFAS of all three orthogonal components and the geometrical mean of the horizontal (GM).

The sensitivity of the SGMSM to each physical variable was assessed based on the computation of the Spearman correlation coefficient between the model input (set of source and path parameters) and the output ($\widetilde{SFAS}_{sim}$). If the correlation is high, then the input parameter has significant impact on the considered output. As an example, the data points computed for the stress drop variable, are presented in Figure 4.

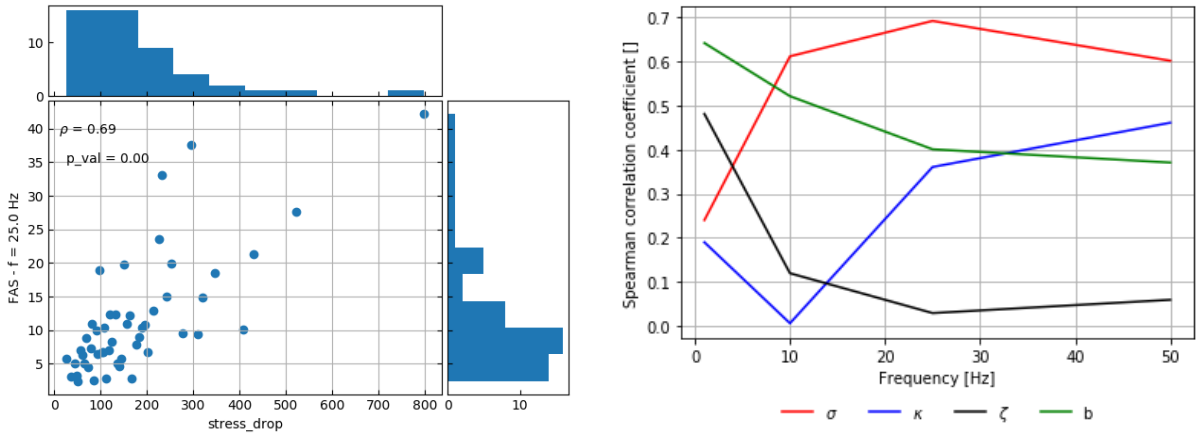

(a) (b)

Fig. 4 - (a) Stress drop vs $\widetilde{SFAS}\widetilde{SFAS}$ for 20.0 Hz, GM component (b) – Stress drop vs $\widetilde{SFAS}\widetilde{SFAS}$ for 20.0 Hz, GM component

Figure 4-(b) summarizes the correlation coefficients of all assessed physical variables for the geometrical mean of the horizontal components. Unsurprisingly, the figure evidences that the correlation coefficient strongly depends on the frequency range. The stress drop and the site attenuation parameter kappa were found to be essential for the higher frequency range, whilst parameters such as the geometrical spreading function exponent and the pulsing percentage of the fault were more so for the shorter frequency range. These observations coincide with those found by other authors researching other more known SGMSM [6], [14], [15], etc.

- Model parameters identification

Identification of the set of physical variables producing the simulations closest to the reference events, or calibration of the SGMSM, was performed using a Bayesian Optimization algorithm.

The optimization algorithm focuses on solving the problem of optimizing a function $g(x)$, such that:

$$\min_{x \in A} g(x) \qquad (6)$$

Where x represents a set of parameters part of the feasible space A . The algorithm consists of two main parts, the definition of a statistical model adjusting the objective function, and an acquisition function leading the decision of where to sample next.

For our application $g(x)$ was defined as the accumulated difference between $\widetilde{SFAS}_{sim}$, and the smoothed Fourier Amplitude Spectrum of the reference, $SFAS_{ref}$ for the range of frequencies valid in the inter-frequency correlation structure defined by Bayless and Abrahamson (2019), $0.1Hz < f < 25.0\ Hz$.

$$g(x) = \sum_{ref} \sum_{f} \left(\log \left(\frac{SFAS_{ref}}{\widetilde{SFAS}_{sim}} \right) \right)^2 \quad (7)$$

A Gaussian process, constructed based on a *Matern* kernel was used to express a Bayesian posterior probability distribution after each evaluation of $g(x)$. The selection of new sampling points based on the statistical model fitted to the evaluations was based on an *expected improvement* function. Further details on Bayesian Optimization algorithms may be found in the literature, [16].

3.2) Frequency content evaluation

Simulations were performed for each of the reference records. A total of 50 simulations where conducted, using as input the given hypocenter and the station locations. No information on the specific faults producing each reference event was sought, therefore we considered a random dip and strike for each simulation, as for the dimensions of the fault we assumed them to be dependent on M_w, based on empirical relationships found in the literature, [17]. These assumptions are expected to affect the dispersion of the results, but since a large number of simulations is performed for each reference record, we expect no important deviation from the mean. Other physical parameters, apart from the geometrical properties of the fault and the location of the site and hypocenter were selected based on the identification algorithm discussed on the previous section of this document.

Table 2. Calibrated physical variables describing the reference record set

Stress drop ($\sigma\sigma$)	125.0 bar
High frequency attenuation (κ_0)	0.02 s
Pulsing Percentage (ζ)	43.95%
Geometrical attenuation (b)	-0.70

The physical variables best describing the SFAS of the reference events, shown in Table 2, agree with those found by previous SGMSM based studies for the Japanese seismogenic environment [18]. The following figure shows the acceleration time histories and SFAS of one the reference events and one if its correspondent simulations.

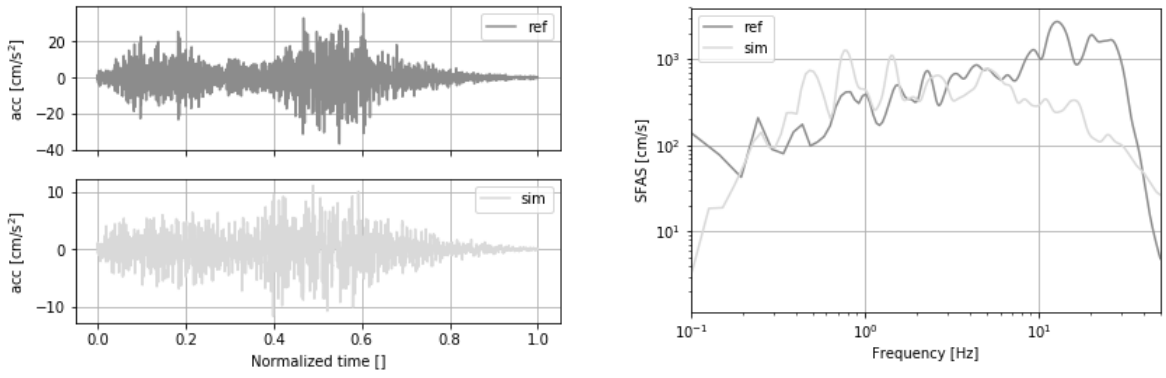

(a) (b)

Fig. 5 - Single simulation comparison (cropped, time normalized signals), TCGH17-04: (a) Time histories, (b) SFAS

Figure 5-(a) summarizes the SFAS comparison of reference and mean simulated events ($log(SFAS_{ref}/SFAS_{sim})$ $log(SFAS_{ref}/SFAS_{sim})$), for the geometrical mean (GM) of the horizontal

components. Overall, the results indicate that the model is able to describe the mean SFAS of the reference set of events, furthermore, high variability was noted for all frequencies of interest, though this was expected due to the included uncertainty in the characterization of the seismic source.

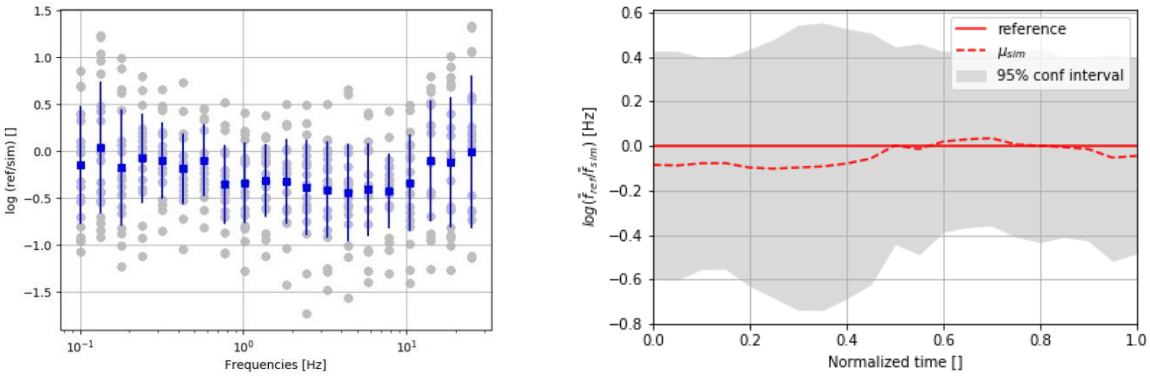

(a) (b)

Fig 5 - (a) SFAS comparison for the whole set, GM component - (b) Instantaneous frequency comparison for the whole set, GM component

Much like the SFAS validation exercise, we expressed the comparison of the instantaneous frequencies as the logarithm of the reference and simulated events ($log(\tilde{f}_{ref}/\tilde{f}_{sim})$), Figure 5-(b). The results demonstrate the method is also, in average, capable of capturing the frequency content evolution noticed in the reference set of events. The larger differences were observed in the initial sections of the signals, indicating that SGMSM description of *P*-waves is not as accurate as that of the *S*-waves. As for the SFAS evaluation, large dispersion was observed for all normalized instants of the signals, this statement becomes more evident if we observe the records individually.

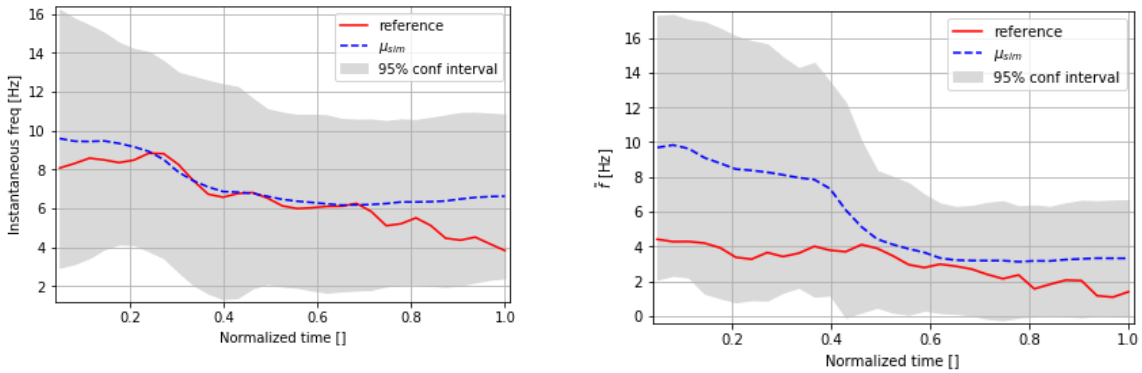

(a) (b)

Fig 6 - (a) Instantaneous frequency TCGH17-01, GM component - (b) Instantaneous frequency FKSH15-02, GM component

Figure 6 shows the individual comparison of the instantaneous frequency for two of the records of the reference set, TCGH17-01 and FKSH15-02, showing the best and the worst fit for the reference set, respectively. Unsurprisingly, large variability was also noticed between the instantaneous frequency functions for the different reference records, however, the latter was consistently captured by the 95% percent confidence interval of the simulations.

When assessing the vertical component (Figure 7) we noted a much poorer performance, both in terms of the mean fit and the dispersion of the results. In other words, for this case study, the SGMSM was not capable of capturing the frequency content of the vertical component when calibrated by the GM component. The error presented in Figure 7-(a) consistently increases with the duration of the signal, indicating an overestimation of the frequency content by the SGMSM.

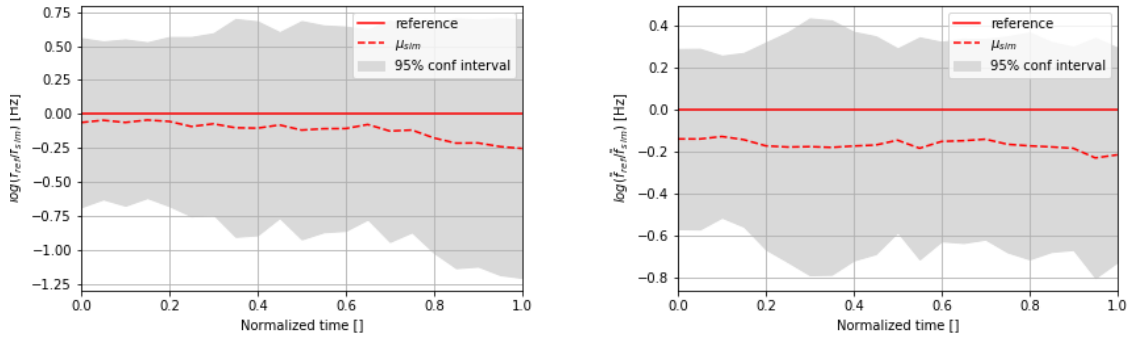

(a) (b)

Fig 7.- (a) Instantaneous frequency comparison for the whole set, vertical component - (b) Instantaneous frequency comparison for the whole set, vertical component, no inter-frequency correlation

To evaluate impact of the inter-frequency correlation structure in the instantaneous frequency, the parameter identification algorithm was re-run for the SGMSM not including the correlation structure. Figure 7-(b) shows the comparison of the instantaneous frequency for the normalized reference and simulated sets. Overall, we noted a consistent increment in the mean error, reaching a maximum logarithmic ratio of -0.21 (*ref/sim = 0.61*), moreover, the dispersion of the results is consistently higher for the last half of the normalized time.

4. Conclusions

The modified Otarola method was found to properly describe the mean frequency content ($SFAS$) of the set of reference ground motions. The method was also found to be able to describe the mean instantaneous frequency ($\tilde{f}$) of the reference signals, capturing the observed instantaneous frequency within the 95% confidence interval for all ground motions. Overall, large dispersion was consistently found through the results. The uncertainty in the seismogenic source (geometry of the fault) caused great part of this dispersion, proper description of the media could constrain the results much more, however, we acknowledge by the analysis of the reference set that the frequency content of ground motion is by nature uncertain.

We noted that the omission of the inter-frequency correlation model lead to consistent higher errors in the instantaneous frequency of the simulated signals. An almost constant over-prediction factor of 0.60 (linear scale) was found throughout the entire normalized duration of the signal.

Parameter identification of the SGMSM, based on the geometrical mean of the horizontal components, leads to poor representation of the frequency content in the vertical component. The increasing error in the vertical component could be explained by the incomplete wave-field of the model, which assumes no different underline spectra for coda-waves.

5. Acknowledgements

The authors acknowledge the economic support for this project by the IUSS - Pavia UME doctorate and the Association Nationale Recherche Technologie (ANRT) through the CIFRE scholarship no 2018/1693.

6. Copyrights

7. References

[1] C. Otarola and S. Ruiz, "Stochastic generation of accelerograms for subduction earthquakes," *Bulleting of the Seismological Society of America,* pp. 2511-2520, 2016.

[2] C. Otarola, J. Ojeda, C. Patensen and S. Ruiz, "Stochastic strong motion simulation in borehole and on surface for the Mw 9.0 Tohoku-Oki 2011 megathrust earthquake considering P, SV and SH amplification transfer functions," *Bulletin of the Seismological Society of America,* 2018.

[3] J. Bayless and N. Abrahamson, "Evaluation of the interperiod correlation of Ground-Motion Simulations," *Bulletin of the Seismological Society of America,* pp. 3413-3430, 2018.

[4] D. Boore, "Stochastic Simulation of High-frequency Ground Motions Based on Seismological Models of Radiated Spectra," *Bulleting of the Seismological Society of America,* pp. 1865-1894, 1983.

[5] D. Boore, "Simulation of ground motion using the stochastic method," *Pure and applied geophysics,* pp. 635-676, 2003.

[6] D. Boore, "Comparing stochastic Point-Source and Finite-Source Ground Motion Simulations: SMSIM and EXSIM," *Bulletin of the Seismological Society of America,* pp. 3202-3216, 2009.

[7] J. Bayless and N. Abrahamson, "An empirical Model for the Interfrequency Correlation of Epsilon for Fourier Amplitude Spectra," *Bulletin of the Seismological Society of America,* 2019.

[8] H. Ghofrani, G. Atkinson and K. Goda, "Implications of the 2011 M 9.0 Tohoku Japan earthquake for the treatment of site effects in large earthquakes," *Bulletin of Earthquake Engineering,* 2012.

[9] L. Burks and J. Baker, "Validation of Ground-Motion Simulations through Simple Proxies for the Response of Engineered Systems," *Bulletin of the Seismological Society of America,* pp. 1930-1946, 2014.

[10] N. Bijelic, T. Lin and G. G. Deierlein, "Validation of the SCEC Broadband Platform simulations for tall building risk assessments considering spectral shape and duration of the ground motion," *Earhtquake Engineering and Structural Dynamics,* pp. 2233-2251, 2018.

[11] K. Konno and T. Ohmachi, "Ground-motion characteristics estimated from spectral ratio between horizontal and vertical components of microtremor," *Bulleting of the Seismological Society of America,* pp. 228-241, 1998.

[12] National Research Institute for Earth Science and Disaster Resilience, *NIED K-NET,* Ibaraki: National Research Institute for Earth Science and Disaster Resilience, 2019.

[13] D. Boore and J. Bommer, "Processing of strong-motion accelerograms: needs, options and consequences," *Soil Dynamics and Earthquake Engineering,* pp. 93-115, 2005.

[14] H. Ghofrani, G. Atkinson, K. Goda and K. Assatourians, "Stochastic Finite-Fault Simulation of the 2011 Tohoku, Japan Earthquake," *Bulletin of the Seismological Society of America,* pp. 1307-1320, 2013.

[15] G. M. Atkinson, D. M. Boore, K. Assatourians, K. Campbell and D. Motazedian, "A guide to differences between stochastic point source and stochastic finite fault simulation methods," *Bulletin of the Seismological Society of America,* pp. 3192-3201, 2009.

[16] P. Frazier, "A tutorial on Bayesian Optimization," Cornell University, Ithaca, NY, 2018.

[17] D. Wells and K. Coppersmith, "New Empirical Relationships among Magnitude, Rupture Length, Rupture Width, Rupture Area, and Surface Displacement," *Bulletin of the Seismological Society of America,* pp. 974-1002, 1994.

[18] G. M. Atkinson and K. Assatourians, "Implementation and Validation of EXSIM (A Stochastic Finite - Fault Ground - Motion Simulation Algorithm) on the SCEC Broadband Platform," *Seismological Research Letters,* 2015.

[19] S. Rezaeian and A. Der Kiureghian, "Stochastic Modelling and Simulation of Groun Motions for Performance-Based Earthquake Engineering," Pacific Earthquake Engineering Research Center, California, 2010.

